Volume loss and soil dilatancy

Markus Maehr*, Ivo Herle**

Summary

Grouting of the tail gap is a usual practise in shield tunnelling. It is often believed that this procedure can reverse or at least reduce the settlement trough above the tunnel. This view can be supported by numerical simulations with a simple elasto-plastic (Mohr-Coulomb) model. However, using a more realistic hypoplastic constitutive equation it can be shown that the grouting at first causes additional settlements. This can be explained by the contractant behaviour of drained soil, which appears pronouncedly after deformation reversals.

1. Introduction

Shield heading is increasingly applied in tunnelling within soil. The rigid shield is to protect the excavated cavity until the lining segments have been installed (Fig. 1). Nevertheless, settlements of the surface cannot be completely prevented. Their origins are:

- 3D soil movement ahead of tunnel face,
- overcut due to
  - pitching angle,
  - curve,
  - conicity of the shield,
- closure of the tail gap,
- consolidation and creep.

The settlement due to the soil movement into the face can be controlled by adjusting the support pressure upon the face and the discharge of extracted soil. The closure of the tail gap is counteracted by grouting cement mortar into the gap. The replacement of ground with mortar is not strictly simultaneous with excavation, so that we can conceive this process rather as a closure of the tail gap followed (more or less soon) by an expansion of this gap by grouting. It is, however, observed that this closure-expansion cycle does not annihilate the surface settlement [Jancsecz *et al.*, 2001]. This is so even if the volume of the grout substantially exceeds the volume of the tail gap. This peculiar phenomenon can be easily explained if we look at the behaviour of drained soil at cyclic loading.

2. Behaviour of soil at cyclic loading

We first consider the stress path of a soil element adjacent to the tunnel (see Fig. 2). This stress path can be simulated by means of laboratory tests, i.e. triaxial or biaxial (= plane deformation) tests, as they are usually applied in soil mechanics laboratories. Figure 3 shows some typical results. A very important issue is that the grouting of the tail gap implies a reversal of the loading path that results from tunnel excavation.

One should pay attention to the dilatancy behaviour of sand. During (triaxial) loading dense sand exhibits first contractancy and later dilatancy. As known, dilatancy is the increase of volume (and, consequently, also of void ratio) that occurs during shearing. Of paramount importance is what happens at reversals of the deformation, i.e. at loading-unloading transitions. Owing to the incremental non-linearity of sand, the unloading is characterised by a much higher stiffness, as refers to the stress-strain curve. Considering the evolution of volumetric strain, it is observed that the previous dilatancy is reversed to contractancy, the rate of which is *much higher* than the one of dilatancy (Fig. 3 right). This fact implies the following result: A loading-unloading cycle leaves behind a compaction of the soil. This is the reason why the cycle consisting of (i) closure of the tail gap, (ii) expansion of the tail gap (by means of grouting) produces a net compaction of the overlaying soil in such a way, that the ground surface exhibits a settlement trough despite of grouting. Interestingly, this fundamental behaviour of soil is *not* modelled by most of the constitutive equations implemented in standard FEM codes. E.g. the so-called Mohr-Coulomb elasto-plastic constitutive equation predicts the behaviour shown in Figure 4: the soil exhibits dilatancy at loading and also immediately after the reversal from loading to unloading, which is fundamentally wrong. Whereas the hypoplastic constitutive equation reproduces this effect realistically (see Fig. 5).

* Institute of Geotechnical and Tunnel Engineering, University of Innsbruck

** Institute of Geotechnical Engineering, TU Dresden

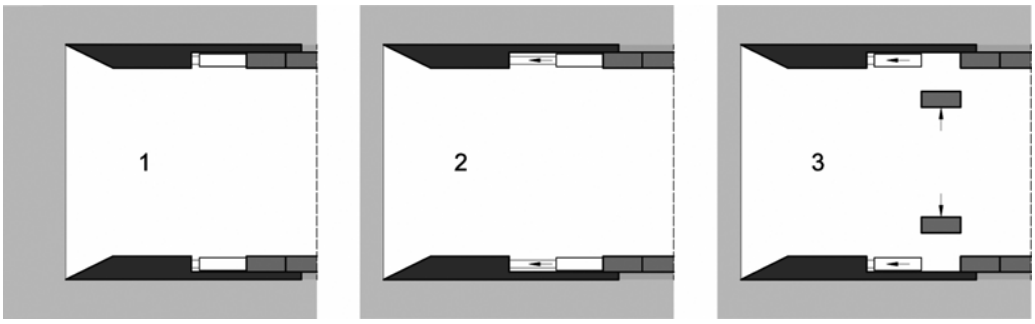

Fig. 1 – The shield is pushed ahead and leaves behind the tail gap.
Fig. 1 – Lo scudo viene spinto in avanti lasciandosi alle spalle l'intercapedine di scavo.

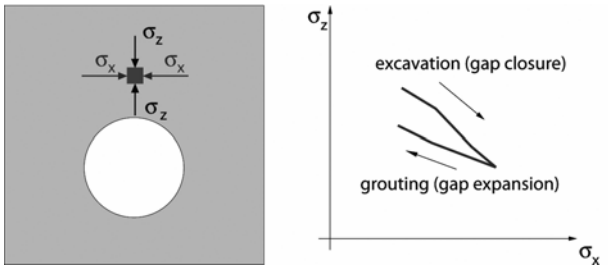

Fig. 2 – Stress path above the crown due to tunnel excavation.
Fig. 2 – Percorso di sforzo sopra la calotta indotto dallo scavo della galleria.

2.1. Hypoplasticity as a realistic model of soil behaviour

Hypoplastic constitutive models [e.g. KOLYMBAS *et al.*, 1995; GUDEHUS 1996] are represented by a single tensorial equation which describes the evolution of stress, i.e. the stress rate, as a function of the effective stress, deformation rate and void ratio. In hypoplasticity, strains are not split into elastic and plastic parts. Consequently, yield and potential surfaces and hardening rules do not need to be formulated. The hypoplastic equations predict different stiffnesses at loading and unloading and take into account changes of mean pressure and density (barotropy and pyknotropy). The stress-induced anisotropy is realistically captured as well.

Hypoplastic laws have been mainly developed to describe the stress-strain behaviour of sands. Numerous calculations of boundary value problems including class-A predictions confirm the suitability of the model for numerical simulations of geotechnical tasks. For a more thorough discussion and additional references, we refer to KOLYMBAS [2000]. In the present work the version of von WOLFFERSDORFF [1996] has been used.

3. Numerical analysis

Several FE-calculations with hypoplasticity and Mohr-Coulomb demonstrate the inability of the latter to simulate the behaviour of soil for nearly cyclic

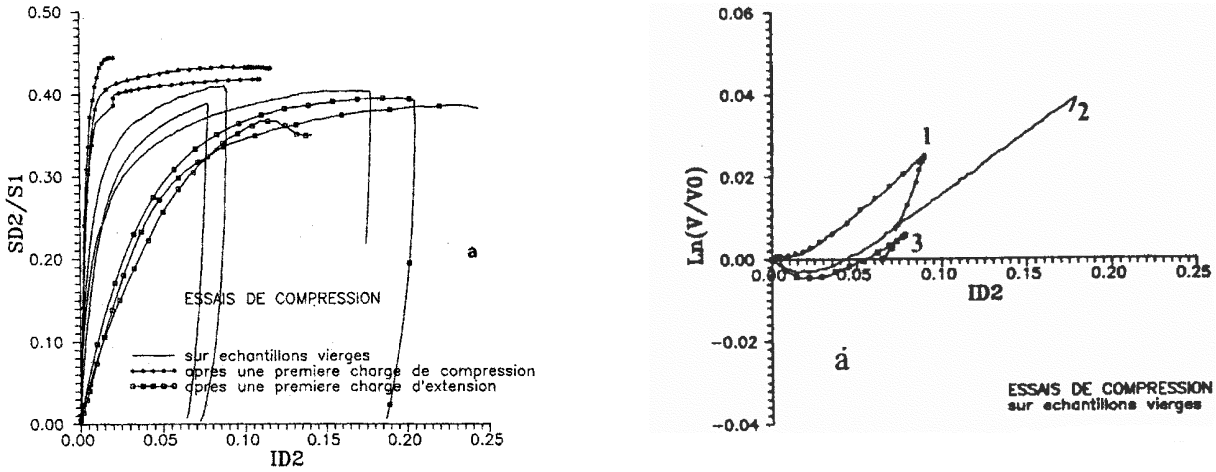

Fig. 3 – Triaxial experiments under different stress paths with Hostun Sand [LANIER *et al.*, 1991]. Note the pronounced contractancy upon unloading (right Figure).
Fig. 3 – Esperimento triassiale lungo differenti percorsi di carico eseguito su sabbia di Hostun [Lanier et al., *1991]. Si noti la pronunciata compattazione in corrispondenza degli scarichi (figura di destra).*

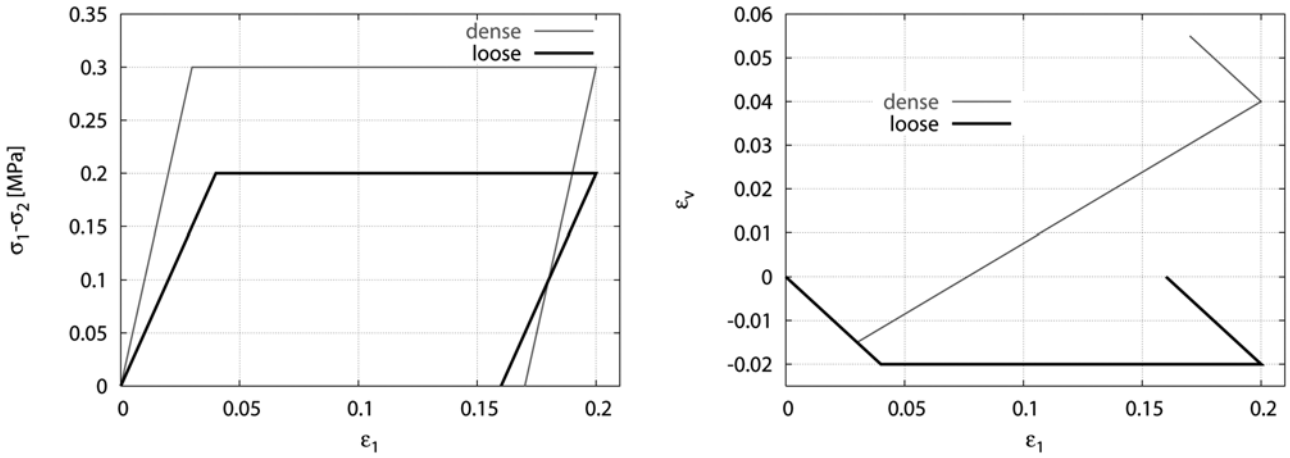

Fig. 4 – Simulation of triaxial test results (left: stress deviator vs. axial strain, right: volumetric strain vs. axial strain) with the Mohr-Coulomb constitutive model.
Fig. 4 – Simulazioni numeriche di prove triassiali drenate di compressione standard (sinistra: sforzo deviatorico-deformazione assiale; destra: deformazioni volumetriche-deformazioni assiali) ottenute mediante modello elasto-plastico perfetto con criterio di rottura alla Mohr-Coulomb.

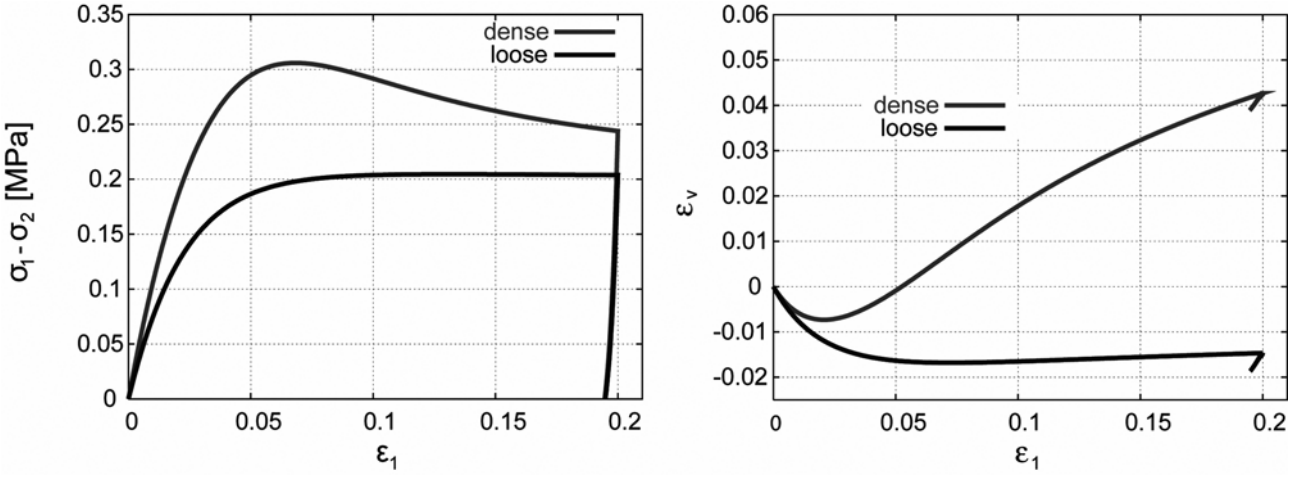

Fig. 5 – Simulation of triaxial test results (left: stress deviator vs. strain, right: volumetric strain vs. strain) with the constitutive model of hypoplasticity. Note that the contractancy upon unloading is correctly modelled.
Fig. 5 – Simulazioni numeriche di prove triassiali drenate di compressione standard (sinistra: sforzo deviatorico-deformazione assiale; destra: deformazioni volumetriche-deformazioni assiali) ottenute mediante un modello ipoplastico. Si noti che la compattazione del materiale in fase di scarico viene colta correttamente.

loading as in a tunnelling problem. A simple model has been chosen, which is not intended to simulate the entire soil-shield interaction nor to predict the behaviour of the lining, but merely to show the importance of a realistic constitutive law for the considered problem of gap grouting.

3.1. Determination of the model parameters

Figures 6 and 7 represent results of standard triaxial and oedometer tests with Hochstetten sand from the vicinity of Karlsruhe in Germany [VON WOLFFERSDORFF, 1996], which were used for the determination of the material parameters of the hypoplastic model [HERLE and GUDEHUS, 1999]. The initial relative density based on the void ratio has been chosen as

$$I_e = \frac{e - e_{\min}}{e_{\max} - e_{\min}} = 0.5.$$

The parameters of the Mohr-Coulomb model were adjusted as a best fit to the results of the triaxial experiments at σ_0 = 0.1 MPa (Fig. 6), obtaining Young's modulus E_0 = 22 MPa, friction angle φ = 33, Poisson's ratio ν=0.3 and dilatancy angle ψ=30.

The Young's modulus E was varied with depth z according to a pressure-dependent scaling law proposed by OHDE [1939], with α set to 0.7:

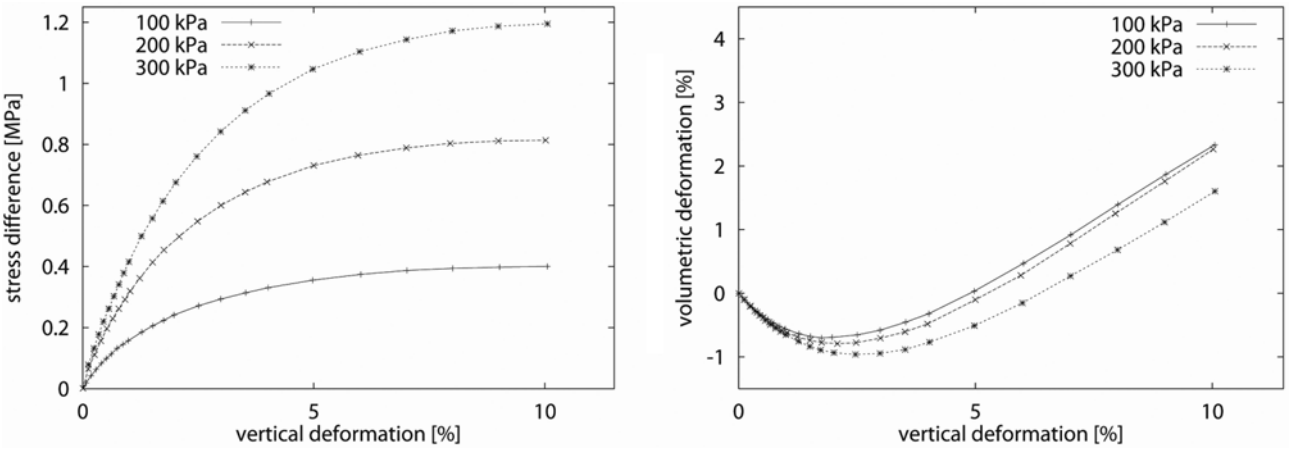

Fig. 6 – Results of standard triaxial tests with Hochstetten sand [VON WOLFFERSDORFF, 1996].
Fig. 6 – Risultati di prove triassiali drenate di compressione standard su sabbia di Hochstetten [VON WOLFFERSDORFF, 1996].

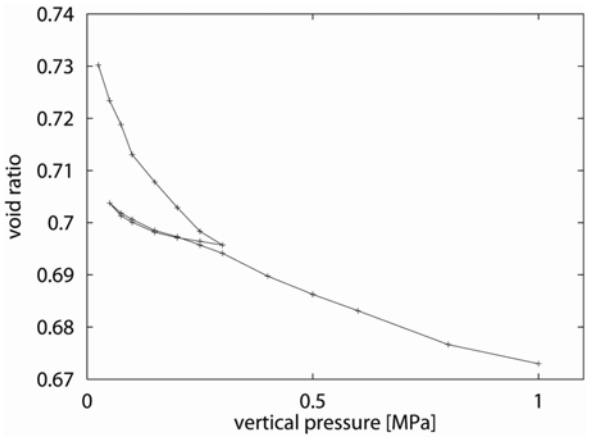

Fig. 7 – Results of an oedometer test with Hochstetten sand [VON WOLFFERSDORFF, 1996].
Fig. 7 – Risultati di una prova edometrica su sabbia di Hochstetten [VON WOLFFERSDORFF, 1996].

$$E(z) = E_0 \left(\frac{\sigma_z(z)}{\sigma_0} \right)^{\alpha} \qquad (1)$$

The resulting Young's moduli are plotted in Figure 8.

The elastoplastic and hypoplastic parameters are summarized in Table I and Table II, respectively.

The calculations have been carried out with the FEM program ABAQUS. Mohr-Coulomb law is a standard part of this FE-package, whereas hypoplasticity has to be implemented by a user-subroutine. In this work the user constitutive model subroutine ('UMAT') by FELLIN and OSTERMANN [2002] has been used, which provides a consistent tangent operator including error control.[1] The boundary conditions and the mesh have been chosen as illustrated in Figure 9. The sequence of the applied deformation is shown in figures 10 to 12. We start from a circular tunnel with 5 m radius (Fig. 10) and apply a convergence of 7 cm (Fig. 11) in order to simulate the excavation. In the second step the tunnel cavity is expanded as displayed in Figure 12.

The calculations have been carried out with the hypoplastic constitutive equation as well as with the Mohr-Coulomb model. To analyse the influence of the dilatancy angle ψ in the Mohr-Coulomb model, which in reality depends on pressure and density, calculations with three different values of ψ have been performed.

3.2. Results of the numerical simulations

3.2.1. HYPOPLASTICITY

Figure 13 shows the evolution of the settlement trough. One can clearly see, that the trough is not annihilated by the cavity expansion – in agreement with field observations. This behaviour is also reflected in the evolution of vertical displacements along the vertical symmetry axis in Figure 14. There, a loosening zone about 2 m above the crown can be identified. It is located at the boundary of the soil arch created during the tunnel convergence. This loosening zone is also shown in a contour plot of void ratios at the end of the convergence-expansion cycle (Fig. 15). Despite the enduring loosening zone the volume loss still increases during gap expansion (Fig. 16).

3.2.2. MOHR-COULOMB

In contrast to the settlement troughs calculated with hypoplasticity, the settlement trough obtained with the Mohr-Coulomb model (Fig. 17) is nearly annihilated by the cavity expansion. Moreover, about 30 m beside the symmetry axis a heave can be observed. This is also depicted in Figure 16, where the volume loss is plotted against tunnel convergence.

Tab. I – Parameters of the Mohr-Coulomb model for Hochstetten sand.
Tab. I – Parametri del modello alla Mohr-Coulomb per la sabbia di Hochstetten.

φ[]	E_0 [MPa]	v	ψ[]
33	58	0.3	30

Tab. II – Parameters of the hypoplastic model for Hochstetten sand.
Tab. II – Parametri del modello ipoplastico per la sabbia di Hochstetten.

ψ_c []	h_s [MPa]	n	e_{d0}	e_{c0}	e_{i0}	a	b
33	1000	0.25	0.55	0.95	1.05	0.25	1.50

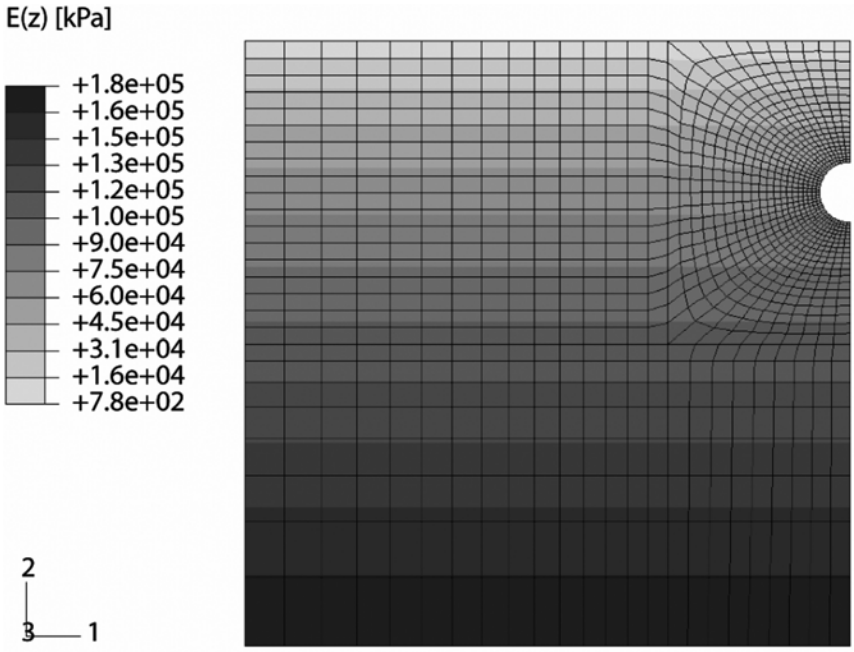

Fig. 8 – Variation of Young's modulus *E*.
Fig. 8 – Variazione del modulo di Young E.

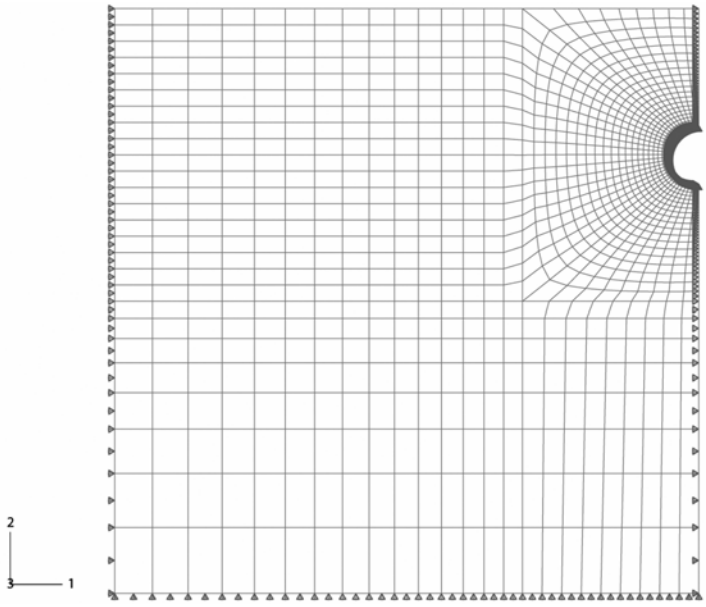

Fig. 9 – Boundary Conditions.
Fig. 9 – Condizioni al contorno.

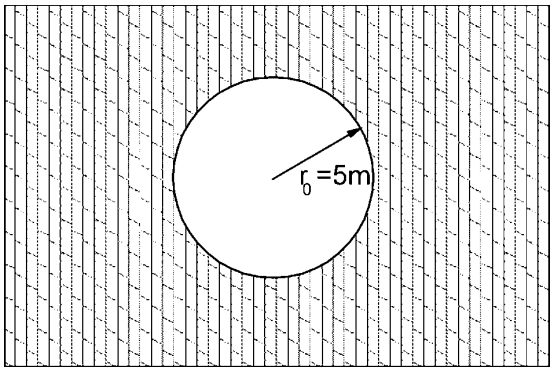

Fig. 10 – Initial configuration.
Fig. 10 – Configurazione iniziale.

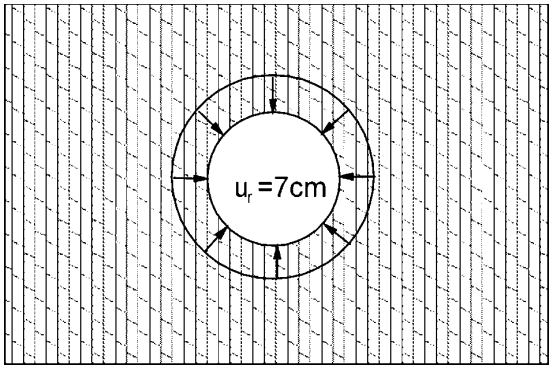

Fig. 11 – Convergence.
Fig. 11 – Convergenza.

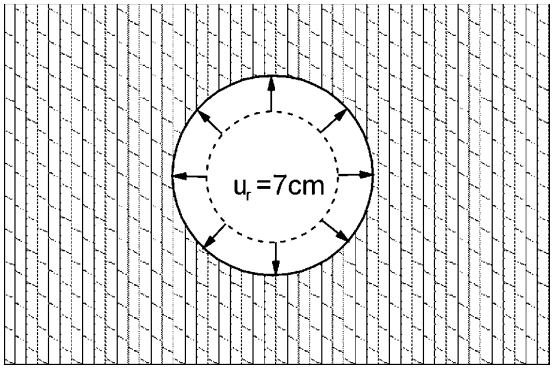

Fig. 12 – Expansion.
Fig. 12 – Espansione.

While the volume loss computed with the hypoplastic material law is still increasing during gap expansion, the volume loss computed with Mohr-Coulomb decreases during expansion. In fact – depending on the angle of dilatancy – one even gets a net volume increase.

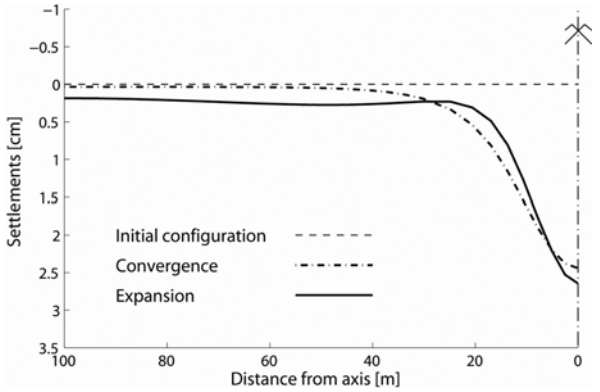

Fig. 13 – Evolution of the settlement trough, hypoplasticity.
Fig. 13 – Andamento dei cedimenti ottenuti mediante il modello ipoplastico.

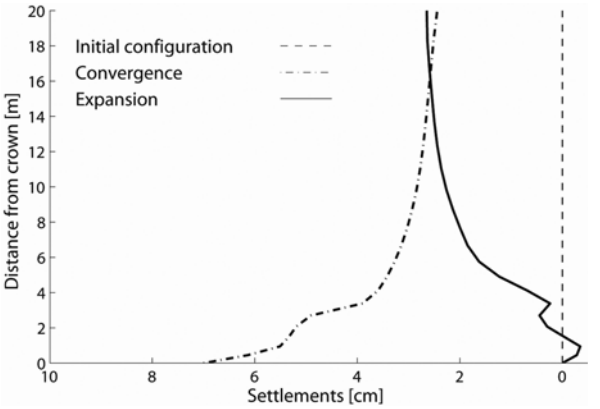

Fig. 14 – Evolution of vertical displacements along the vertical symmetry axis, hypoplasticity.
Fig. 14 – Andamento degli spostamenti verticali lungo l'asse verticale di simmetria. Simulazioni ottenute mediante il modello ipoplastico.

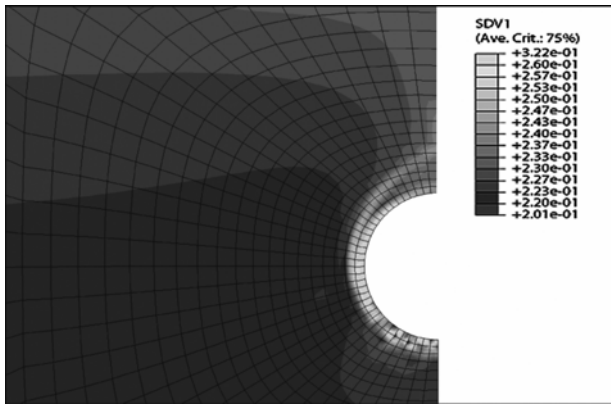

Fig. 15 – Void ratio.
Fig. 15 – Indice dei vuoti.

4. Model tests

As there are only few field data available regarding settlement troughs in sandy soil, laboratory tests have been carried out to deliver additional insight to soil behaviour during shield tunneling. Figure 19 shows a photograph of the model used to simulate tail gap grouting, which represents a plane strain section. Here again the main focus of the test was merely put on investigating the volumetric soil be-

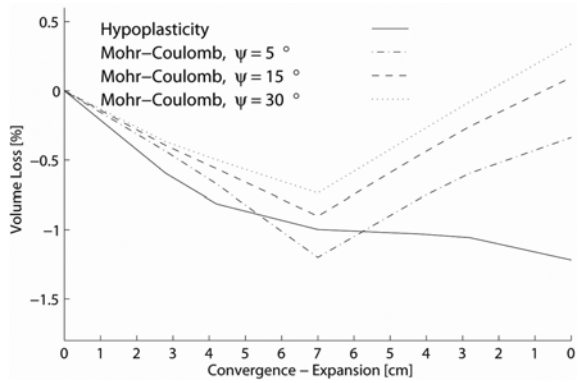

Fig. 16 – Evolution of volume loss with the change of the cavity radius.
Fig. 16 – Evoluzione della perdita di volume al variare del raggio della cavità.

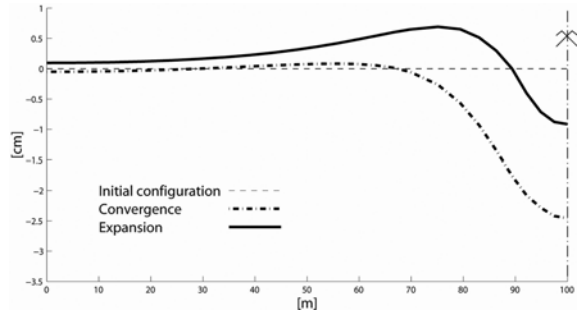

Fig. 17 – Evolution of the settlement trough, Mohr-Coulomb.
Fig. 17 – Evoluzione dei cedimenti: simulazioni numeriche ottenute mediante legame elasto-plastico perfetto con criterio di rottura alla Mohr-Coulomb.

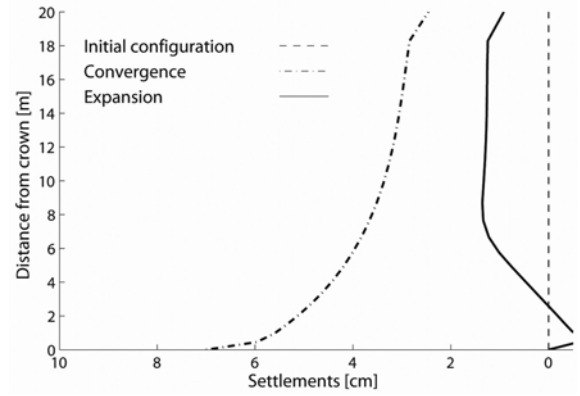

Fig. 18 – Evolution of vertical displacements along the vertical symmetry axis, Mohr-Coulomb law, ψ=30.
Fig. 18 – Evoluzione degli spostamenti verticali lungo l'asse di simmetria, simulazioni numeriche, criterio di rottura alla Mohr-Coulomb, ψ=30.

haviour rather than on simulating the entire soil-shield interaction.

The process of tunneling corresponds to the numerical model. In the first step the diameter of the cylinder is reduced from 17 cm to 16.3 cm to simulate convergence. In the second step it is enlarged back to 17 cm (simulating tail gap grouting). The overburden reaches 34 cm. Assuming a scale of 1/50 this corresponds to a tunnel of 8.50 m diameter having a tail gap of 17.5 cm and 17 m (=2*D*) overburden. The cylinder is elastically supported in vertical direction and fixed in horizontal direction. The diameter of the cylinder can be varied smoothly (see Fig. 20).

Fig. 19 – Test setup.
Fig. 19 – Apparecchiatura di prova.

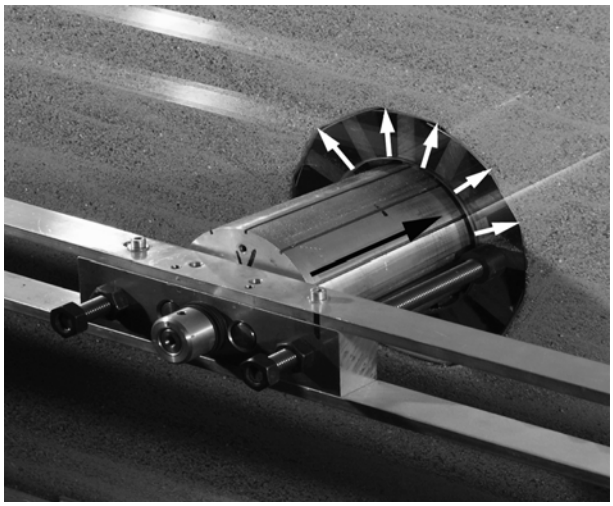

Fig. 20 – Cylinder with variable diameter.
Fig. 20 – Cilindro a diametro variabile.

Ground movements were measured in two ways. Settlements of the sand surface were measured by infrared sensors linked with a step motor. Ground movements around the cylinder were obtained by numerical processing of digital images captured using a digital camera. The analysis was performed using MatPIV, a free available PIV (Particle image velocimetry) program[2], running within Matlab. Particle image velocimetry enables calculation of movements without using marker beads. Further details of the experimental procedure are given by FROMM [2002] and MAEHR (to appear).

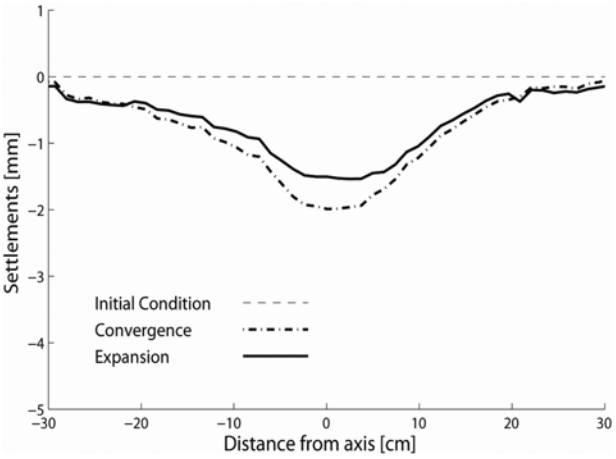

Fig. 21 – Settlements measured in the model test.
Fig. 21 – Cedimenti misurati con il modello sperimentale.

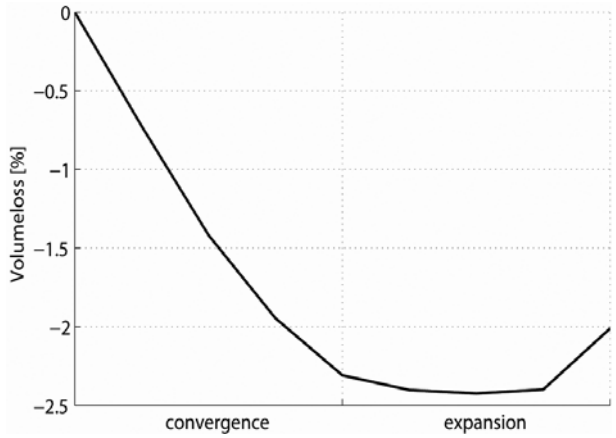

Fig. 22 – Volume loss from the model test.
Fig. 22 – Perdita di volume ottenuta con il modello sperimentale.

Figure 21 shows surface settlements obtained in the test v280404. Qualitatively the behaviour coincides with the Finite-Element calculations (cf. Fig. 15 and Fig. 21)[3]. The settlements increase with decreasing diameter (convergence) and they remain nearly constant when the diameter increases again (closure of the gap).

The volume loss remains nearly constant during the expansion of the cylinder (see Fig. 22). Only at the end of the expansion slight upheavals occur.

5. Conclusions

The settlement due to tail gap closure can not be completely revoked with grouting from the very beginning – apart from excessive grouting. This is due to the contractancy of soil at loading-unloading cycles and has been simulated with finite elements and the hypoplastic constitutive equation. The comparison of the settlement trough obtained using elasto-plasticity and the one obtained with hypoplasticity points out to the advantage of realistic constitutive laws. Laboratory model tests reveal qualitatively good agreement with the finite element calculations using hypoplasticity.

Note

[1] The UMAT is available on http://www.geotechnik.uibk.ac.at.

[2] The programm is available under: http://www.math.uio.no/jks/matpiv/.

[3] The soil parameters of the FE-calculation have not been adopted to the tests.

References

FELLIN W. and OSTERMANN A. (2002) – *Consistent tangent operators for constitutive rate equations*. Int. J. for Numer. Anal. Meth. Geomech., 26, pp. 1213-1233.

FROMM H. (2002) – *Experimentelle Ueberpruefung von Oberflaechensetzungen infolge Ringspaltes und seiner Verpressung. Master's thesis*. University of Innsbruck.

GUDEHUS G. (1996) – *A comprehensive constitutive equation for granular material*. Soils and Foundation, 36, 1, pp. 1-12.

HERLE I. and GUDEHUS G. (1999) – *Determination of parameters of a hypoplastic constitutive model from properties of grain assemblies*. Mechanics of Cohesive-Frictional Materials, 4, 5, pp. 461-486.

JANCSECZ S., FRIETZSCHE W., BREUER J. and ULRICHS K.R. (2001) – *Tunnelbau 2001*. vol. XXV, chapter III. Minimierung von Senkungen beim Schildvortrieb am Beispiel der U-Bahn Düsseldorf, pp. 165-214. Glückauf, Essen.

KOLYMBAS D. (2000) – *Introduction to Hypoplasticity*. Number 1 in Advances in Geotechnical Engineering and Tunnelling. Balkema.

KOLYMBAS D., HERLE I. and VON WOLFFERSDORFF P.-A. (1995) – *Hypoplastic constitutive equation with back stress*. International Journal of Numerical and Analytical Methods in Geomechanics, 19, 6, pp. 415-446.

LANIER J., DI PRISCO C. and NOVA R. (1991) – *Induced anisotropy in Hostun sand: experiments and theoretical analysis*. Rev. Franc. Geotech., 57, pp. 59-74, October 1991.

MAEHR M. *Numerical simulation of shield tunneling*. PhD thesis, University of Innsbruck, to appear.

OHDE J. (1939) – *Zur Theorie der Druckverteilung im Baugrund*. Bauingenieur, 20, pp. 451-459.

VON WOLFFERSDORFF P.-A. (1996) – *A hypoplastic relation for granular materials with a predefined limit state surface*. Mechanics of Cohesive-Frictional Materials, 1, pp. 251-271.

Perdite di volume e dilatanza del terreno

Sommario

Il consolidamento dell'intercapedine presente in corrispondenza del fronte di scavo è una pratica comune nella realizzazione di gallerie mediante scudi. Comunemente si crede che questa procedura possa recuperare o almeno ridurre i cedimenti che si risentono sul piano campagna soprastante la galleria. Questa assunzione è confortata dai risultati numerici ottenuti mediante codici di calcolo agli elementi finiti, all'interno dei quali sono implementati modelli elasto-plastici con criterio di rottura alla Mohr-Coulomb. Al contrario, utilizzando un legame costitutivo ipoplastico in grado di riprodurre il comportamento meccanico del terreno in modo più realistico, è possibile mostrare come anche il grouting, all'inizio, causi dei cedimenti aggiuntivi. Questo può essere spiegato dal comportamento contrattante del terreno, che si manifesta in modo marcato quando viene invertito il processo di carico.